JOURNAL OF SYNCHROTRON RADIATION

ISSN 1600-5775

Examining a synchrotron-based approach for *in situ* analyses of Al speciation in plant roots

Zhigen Li,[a] Peng Wang,[a,b] Neal W. Menzies,[a] Brigid A. McKenna,[a] Chithra Karunakaran,[c] James J. Dynes,[c] Zachary Arthur,[c] Na Liu,[c] Lucia Zuin,[c] Dongniu Wang[c] and Peter M. Kopittke[a]*

[a]School of Agriculture and Food Sciences, The University of Queensland, St Lucia, Queensland 4072, Australia, [b]College of Resources and Environmental Sciences, Nanjing Agricultural University, Nanjing, Jiangsu 210095, People's Republic of China, and [c]Canadian Light Source Inc., 44 Innovation Boulevard, Saskatoon, SK S7N 2V3, Canada. *Correspondence e-mail: p.kopittke@uq.edu.au

Received 26 April 2019
Accepted 21 October 2019

Edited by R. W. Strange, University of Essex, UK

Keywords: Al speciation; *Arabidopsis*; *Fagopyrum tataricum*; *Glycine max*; plant root tissues; XANES; *K*-edge; *L*-edge; tetrahedral coordination; octahedral coordination.

Supporting information: this article has supporting information at journals.iucr.org/s

Aluminium (Al) *K*- and *L*-edge X-ray absorption near-edge structure (XANES) has been used to examine Al speciation in minerals but it remains unclear whether it is suitable for *in situ* analyses of Al speciation within plants. The XANES analyses for nine standard compounds and root tissues from soybean (*Glycine max*), buckwheat (*Fagopyrum tataricum*), and Arabidopsis (*Arabidopsis thaliana*) were conducted *in situ*. It was found that *K*-edge XANES is suitable for differentiating between tetrahedral coordination (peak of 1566 eV) and octahedral coordination (peak of 1568 to 1571 eV) Al, but not suitable for separating Al binding to some of the common physiologically relevant compounds in plant tissues. The Al *L*-edge XANES, which is more sensitive to changes in the chemical environment, was then examined. However, the poorer detection limit for analyses prevented differentiation of the Al forms in the plant tissues because of their comparatively low Al concentration. Where forms of Al differ markedly, *K*-edge analyses are likely to be of value for the examination of Al speciation in plant tissues. However, the apparent inability of Al *K*-edge XANES to differentiate between some of the physiologically relevant forms of Al may potentially limit its application within plant tissues, as does the poorer sensitivity at the *L*-edge.

1. Introduction

Aluminium (Al) is the third most abundant element in the Earth's crust after oxygen (O) and silica (Si) (Sposito, 2008). In soils of near-neutral pH, Al-containing minerals have low solubility and concentrations of soluble Al remain low. However, the solubility of these Al-containing minerals is high in acid soils, with soluble Al often increasing to concentrations that are toxic to plants. Indeed, Al toxicity is an important growth-limiting factor in the acid soils that comprise *ca* 30–40% of the world's arable land (von Uexküll & Mutert, 1995). In Australia alone, for example, acid soils cost AU$1.5 billion per annum in lost productivity, yet it is economically viable to lime only 4% of these soils (Hajkowicz & Young, 2005; NLWRA, 2002). Thus, improving growth in acid Al-toxic soils requires breeding of plants that are either resistant to, or tolerant to, elevated Al. Indeed, given that 97.6% of human food (joules) comes from soil (Brevik & Burgess, 2012), it is also essential that productivity of agricultural soils is maintained in order to feed the increasing human population.

It has been reported that Al exerts a range of toxic effects upon its exposure to plant roots. For example, it has been found that Al causes interference with DNA synthesis and

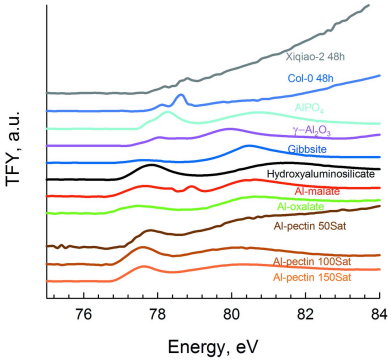

© 2020 International Union of Crystallography

mitosis (Liu *et al.*, 1993), disrupts the function of the Golgi apparatus (Bennet *et al.*, 1985), damages membrane integrity (Ishikawa *et al.*, 2000; Yamamoto *et al.*, 2001) and inhibits mitochondrial functions (Yamamoto *et al.*, 2002). However, the initial (primary) toxic effect of Al is an inhibition of wall loosening (Jones *et al.*, 2006), resulting in a reduction in root elongation rate (RER) within 5 min (Kopittke *et al.*, 2015). Indeed, it is known that >99% of Al accumulates within the cell wall (Taylor *et al.*, 2000) and that the cell wall plays a critical role in the toxicity of Al (Horst *et al.*, 2010; Kopittke *et al.*, 2015; Jones *et al.*, 2006).

Because of the complex nature of the many toxic interactions of Al with plant roots, the identification of novel approaches for examining Al within roots would potentially be of substantial benefit. In this regard, synchrotron-based X-ray absorption spectroscopy (XAS) has the unique advantage of being a non-destructive *in situ* method that can be used to examine elemental speciation. Although an increasing number of studies have utilized this approach to examine elemental speciation in studies of environmental chemistry, the potential use of this technique for determining the speciation of Al in plant tissues has received little attention (Kopittke *et al.*, 2016). Indeed, we are aware of only one study using this approach in Al-exposed plant roots, with Al *K*-edge X-ray absorption near-edge structure (XANES) used to compare speciation of Al in three different samples of root tissues of a tolerant near-isogenic line (NIL, ET8) and a sensitive NIL (ES8) of wheat (*Triticum aestivum*) (Kopittke, McKenna *et al.*, 2017). It was determined that there were differences between the Al coordination of the three samples studied, with the root tissues of ET8 exposed to Al for only 3 h containing more Al in octahedral coordination than the tissues of ES8.

The aim of the present study was to provide a detailed methodological assessment of the usefulness of Al *K*-edge and *L*-edge XAS for the *in situ* comparison of the speciation of Al in root tissues of various plant species. Three plant species were selected: soybean (*Glycine max*), Arabidopsis (*Arabidopsis thaliana*) and buckwheat (*Fagopyrum tataricum*), on the basis that they differ markedly in the mechanisms used to tolerate toxic levels of Al in the rooting medium. The three plant species were grown in media containing toxic levels of Al for 1 to 72 h. The samples were analysed using Al *K*-edge and *L*-edge XAS, with the spectra obtained for the plant root tissues compared with spectra for various Al-containing standard compounds. By examining the potential suitability of XAS for the study of Al speciation in plant tissues, it is hoped that this study will provide useful information for the future investigation of the behaviour of Al within roots exposed to toxic levels of Al.

2. Materials and methods

2.1. Plant growth and measurement of RER

Experiment 1 aimed to provide dose-response curves for the various plants in order to examine their response to toxic levels of Al. Three plant species were examined: soybean (*G. max*, cv. Bunya), buckwheat (*F. tataricum*) and Arabidopsis [*A. thaliana*, wild-type Columbia-0 (Col-0)]. Two varieties were examined for buckwheat (black Tartary buckwheat Heifeng-1 and yellow Tartary buckwheat Xiqiao-2), yielding a total of four different plants. Soybean is known to be comparatively sensitive to Al (Kopittke *et al.*, 2016). As a wild type of Tartary buckwheat, Xiqiao-2 is more sensitive to Al than is Heifeng-1 (Zhu *et al.*, 2015). For Arabidopsis, the wild-type Col-0 is comparatively sensitive to Al (Larsen *et al.*, 2005; Huang *et al.*, 2010).

An initial experiment was undertaken in order to obtain dose-response curves for the various plants. For soybean, the experiment consisted of seven treatments with seven Al concentrations (0, 5, 10, 15, 20, 30 and 50 μ*M* added using $AlCl_3{\cdot}6H_2O$), while, for buckwheat, the experiment consisted of 14 treatments with two plants (two buckwheat varieties) and seven Al concentrations (0, 50, 100, 150, 200, 300 and 400 μ*M*). Each treatment was replicated twice. Soybean and buckwheat seedlings were grown in simple continuously aerated nutrient solutions as described by Kopittke *et al.* (2015), while Arabidopsis was grown in solid culture medium as detailed below. Briefly, for soybean and buckwheat, seeds were germinated in tap water by rolling them in a paper towel suspended vertically for three days. The seedlings were placed in Perspex strips placed across 600 ml beakers filled to the brim (650 ml) with a nutrient solution containing 1 m*M* $CaCl_2$ and 5 μ*M* H_3BO_3 at room temperature (25°C), with pH adjusted to 4.8 using 0.1 *M* HCl. There were seven seedlings per strip, forming one experimental unit. After growth for *ca* 18 h in this basal solution, seedlings were transferred to different beakers containing 1 m*M* $CaCl_2$, 5 μ*M* H_3BO_3 and the Al concentration of interest (above) for a further 48 h. The pH of all Al-containing nutrient solutions was lowered to 4.8 using 0.1 *M* HCl. To enable calculation of root length, images were captured after 0 h (*i.e.* upon transfer to the Al-containing solutions) and after 48 h exposure by removing the strip from the beaker and placing it horizontally beneath a digital camera mounted on a tripod. Root lengths (and hence relative root elongation rate, RRER) were later calculated from the data measured using *ImageJ* version 1.45s which is available at http://imagej.nih.gov/ij/.

For Arabidopsis, seeds were surface sterilized using 8% sodium hypochlorite solution (NaClO) for 15 min. The seeds were then washed three times with sterile deionized water before being placed to germinate on a solid culture medium which consisted of 1 m*M* KNO_3, 1 m*M* $Ca(NO_3)_2$, 0.2 m*M* KH_2PO_4, 1 m*M* K_2SO_4, 2 m*M* $MgSO_4$, 0.25 m*M* $(NH_4)_2SO_4$, 0.5 m*M* $CaSO_4$, 0.2 μ*M* $MnSO_4$, 0.1 μ*M* $CaCl_2$, 0.0005 μ*M* $CoCl_2$, 0.05 μ*M* $CuSO_4$, 2 μ*M* $ZnSO_4$, 0.2 μ*M* $NaMoO_4$, 5 μ*M* H_3BO_3, 0.1% sugar and 2.2% agar (Huang *et al.*, 2010). The solid culture medium was adjusted to pH 5.0 with 0.1 *M* HCl before being sterilized at 121°C for 30 min. After sterilization, the pH of the medium decreased to 4.6. Sealed Petri dishes were maintained at 22°C with 65% relative humidity. After 48 h growth in this basal (Al-free) solid culture media, seedlings were transferred to treatment growth media to which Al

had been added to achieve total concentrations of 0, 10, 50, 200 and 500 μ*M*. Thus, for Arabidopsis, each experiment unit consisted of more than 30 seedlings per Petri dish, with five Al concentrations (0, 10, 50, 200 and 500 μ*M*). Root lengths were recorded after 0 and 48 h using a digital camera. Because of binding of Al by the agar (Sivaguru & Horst, 1998), the final concentration of soluble inorganic monomeric Al was measured with a reaction kinetics approach using pyrocatechol violet as described by Kerven *et al.* (1989). Hereafter, unless otherwise stated, all data presented are for the concentrations of soluble Al measured within the agar, not the total Al added.

2.2. Plant tissue analyses

Experiment 2 aimed to allow for measurement of the Al concentrations in the bulk apical root tissues. For each treatment (each with three replicates), *ca* 50 root apices were required to provide sufficient tissue, with the complete experiment consisting of 12 treatments. For soybean and buckwheat, seedlings were grown in 22 l containers filled with 1 m*M* $CaCl_2$ and 5 μ*M* H_3BO_3 at pH 4.8. After 24 h growth in basal solutions, seedlings were moved to new containers with 1 m*M* $CaCl_2$, 5 μ*M* H_3BO_3 and the desired Al concentration at pH 4.6. The concentration of Al selected was sufficient to reduce RRER by 75% for soybean over 48 h (30 μ*M*), and sufficient to reduce RRER by 25% for buckwheat for Heifeng-1 (120 μ*M*) and for Xiqiao-2 (50 μ*M*). For Arabidopsis, seedlings were grown on solid culture media as outlined earlier. The total Al was added at a concentration of 500 μ*M* (corresponding to a soluble Al concentration of 36 μ*M*, sufficient to reduce RER by 60% after 48 h), with root apical tissues harvested after 48 h.

After exposure for 1 or 48 h, the apical root tissues (10 mm) were rinsed with deionized water, harvested and weighed in 5 ml volumetric flasks. The samples were dried at 65°C before being digested using 1.0 ml of a mixture of nitric acid and perchloric acid (1:5). The flasks were allowed to sit overnight before digesting on a hotplate at up to 250°C. Deionized water was added to each flask to bring the final volume to 5 ml and elemental composition was determined using inductively coupled plasma optical emission spectroscopy.

2.3. Synchrotron-based XANES analyses

Experiment 3 aimed to examine the suitability of synchrotron-based *K*-edge and *L*-edge XANES for examining the speciation of Al within plant root tissues. Plants were grown as described for Experiment 2, with *ca* 50 seedlings required to obtain sufficient material for analyses. Again, soybean seedlings were exposed to 30 μ*M* Al, buckwheat Heifeng-1 to 120 μ*M* Al, buckwheat Xiqiao-2 to 50 μ*M* Al and Arabidopsis to 36 μ*M* Al. Root apical tissues (10 mm) were harvested after 1, 12 and 48 h for soybean, and after 1 and 48 h for buckwheat and Arabidopsis. Upon harvest, all root apical tissues were immediately frozen in liquid nitrogen before being freeze dried for 3 d using a freeze dryer (Benchtop K, VirTis).

The Al *K*-edge XANES spectroscopy was conducted at the spherical-grating monochromator (SGM; 11ID-1) beamline of the Canadian Light Source (Saskatoon, Canada). Root apical tissues were homogenized in a mortar and pestle at room temperature and then pressed evenly on double-sided carbon tape on a Cu holder. The sample chamber was pumped to 10^{-6} Torr (1 Torr = 133.322 pa) and spectra were acquired at the Al *K*-edge from 1550 to 1600 eV using a 10 s slew scan. The spectra presented are the average of 60 scans from different regions within each sample as measured in fluorescence mode using four silicon drift detectors (Amptek). Normalization of the spectra was performed using the I0 spectra (I0 is the incident beam) collected simultaneously from an Au mesh in front of the sample. The energy scale was calibrated using $AlPO_4$ assuming a value of 1566.1 eV.

The Al $L_{2,3}$-edge data were collected at the variable-line-spacing plane-grating monochromator (11ID-2) beamline at the Canadian Light Source. The medium energy grating was used to cover the Al *L*-edge and scans were recorded from 74 to 84 eV with an energy step size of 0.1 eV (Hu *et al.*, 2007). A dwell time of 6 to 20 s per data point was used depending on the signal-to-noise level of samples using a beam size of 100 μm × 100 μm at the exit slits. The total electron yield signal (*i.e.* the drain current from the sample measured with an ampere meter) measures the elemental information tens of nanometres from the surface, while the total fluorescence yield (TFY) measures the elemental information hundreds of nanometres from the surface (measured using a microchannel plate detector), with both being recorded; the TFY data were also used for further analysis (Kasrai *et al.*, 1993). The intensity of the incident beam (I0) was measured using a nickel mesh upstream of the sample chamber and the I0 signal was used to normalize all the sample spectra. In addition, *Origin* was used to fit a linear curve to the sloping pre-edge baseline because of distortion caused by the O 2*s* absorption signal. The sloping baseline of the post-edge was not adjusted. All spectral energy scales were calibrated to the main Al peak of $AlPO_4$ at 78.2 eV (Hu *et al.*, 2008).

The spectra from the samples were compared with reference spectra from nine standard compounds, and the linear combination fitting (LCF) of plant spectra and reference compounds was conducted using *Athena* version 0.9.26 (http://bruceravel.github.io/demeter/). The standard compounds included three commercial compounds [Al–phosphate (Sigma-Aldrich), γ-Al_2O_3 (Alfa Aesar) and gibbsite (reagent grade, synthetic, Wards Natural Science)] and six compounds (hydroxyaluminosilicate, Al–malate, Al–oxalate and Al–pectin prepared with various concentrations of Al) prepared for this study.

To prepare the hydroxyaluminosilicate (Exley & Birchall, 1992), 10 l of 0.1 *M* NaCl was prepared to which 5.7 g of $Na_2SiO_3{\cdot}9H_2O$ was added. The pH was reduced to a value of 3 using 6 *M* HCl, with sufficient $AlCl_3{\cdot}6H_2O$ added to yield an Al concentration of 500 μ*M*. The pH was then increased to 6.0 using 1 *M* NaOH, with the solution left to equilibrate for 7 d. The precipitate (hydroxyaluminosilicate) was collected, briefly rinsed with deionized water and freeze dried. For Al–malate,

stock solutions of 50 m*M* $AlCl_3{\cdot}6H_2O$ and 200 m*M* L-malic acid (Sigma-Aldrich, 112577) were prepared, with 3.63 ml of 1*M* NaOH added to 12.5 ml of L-malic acid before the addition of 10 ml of $AlCl_3{\cdot}6H_2O$. The final pH of this mixture was 4.5. The Al–oxalate standard was prepared in a similar manner using 200 m*M* oxalic acid (Sigma-Aldrich, 247537). Finally, the Al–pectin standards were prepared using pectin from citrus fruit (Sigma-Aldrich, P9436). Sufficient KOH was added to achieve a negative charge of 38 μ*M* COO^- ml^{-1} (McKenna *et al.*, 2010), with a stock solution of 100 m*M* Al added to achieve 50, 100 or 150% saturation. The aqueous/gel standard compounds (Al–malate, Al–oxalate and Al–pectin) were freeze dried before analyses. All samples and standard compounds were spread directly onto the carbon tape for analyses.

3. Results

3.1. Effects of Al on RER and root tissue concentration

In Experiment 1, for all three plant species, RRER decreased as the Al concentration increased (Fig. 1). Soybean was the most sensitive, with 30 μ*M* Al reducing RRER by 75% (and 5 μ*M* reducing RRER by 25%) [Fig. 1(*a*)]. In contrast, buckwheat was the most tolerant, with *ca* 50 μ*M* resulting in a 25% reduction in RRER for Xiqiao-2 and 120 μ*M* resulting in a 25% reduction in RRER for Heifeng-1 [Fig. 1(*b*)]. Although Heifeng-1 was more tolerant of Al than Xiqiao-2, the magnitude of the difference was less than expected from previous studies (Zhu *et al.*, 2015). For Arabidopsis Col-0 it was found that 36 μ*M* Al reduced RRER by 60% [Fig. 1(*c*)].

Experiment 2 provided information on the bulk concentration of Al within the apical root tissues (0–10 mm) when exposed to concentrations resulting in a 75% reduction in RRER over 48 h for soybean, 25% for buckwheat and 60% for Arabidopsis. Despite the markedly different concentrations of soluble Al in the rooting media (ranging from 30 μ*M* for soybean to 120 μ*M* for buckwheat), root apical tissue concentrations were surprisingly similar (Fig. 2). For example, after 48 h exposure, soybean and buckwheat Heifeng-1 accumulated similar Al concentrations, 5.2 mg g^{-1} for soybean and 4.6 mg g^{-1} for Heifeng-1 (Fig. 2, all tissue concentrations on a dry-weight basis). In contrast, for the apical root tissues of the sensitive buckwheat Xiqiao-2, concentrations increased to only 2.0 mg g^{-1} (Fig. 2). For Arabidopsis, concentrations of Al in the apical root tissues were 0.4 mg g^{-1} after 1 h and 3.9 mg g^{-1} after 48 h (Fig. 2).

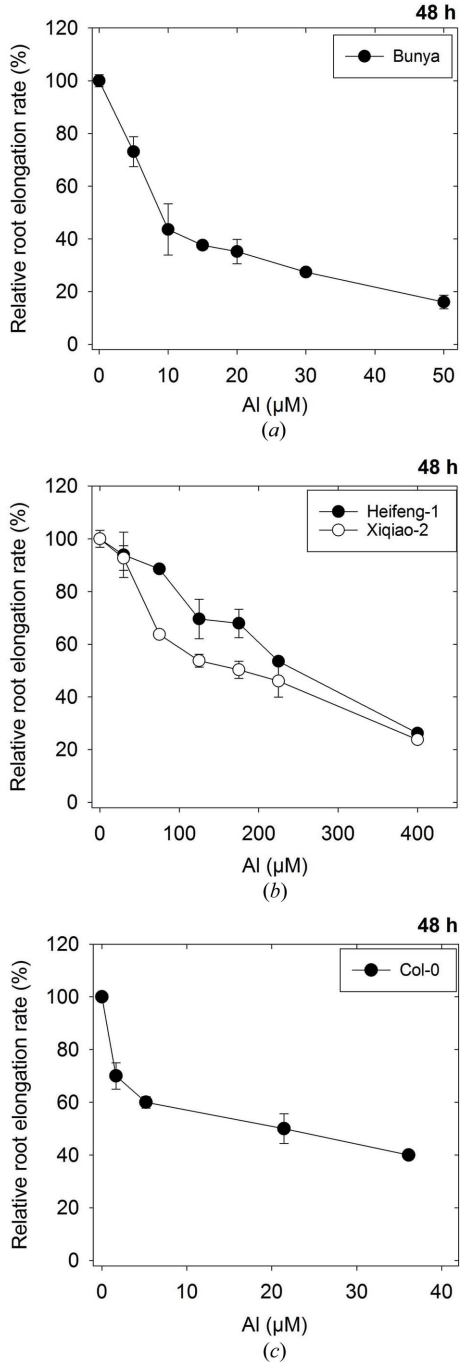

Figure 1
The effect of Al concentration on the RRER of soybean (*a*), buckwheat (*b*) and Arabidopsis (*c*). For soybean and buckwheat, data are the arithmetic means of three replicates (each with seven seedlings). For Arabidopsis, data are the arithmetic means of more than 30 individual seedlings in one Petri dish. Standard deviations are shown.

3.2. Al *K*-edge XANES of standard compounds

It is known that Al *K*-edge XANES is useful for differentiating between Al that is octahedrally coordinated and Al that is tetrahedrally coordinated in minerals (Ildefonse *et al.*, 1998; Li *et al.*, 1995). Specifically, the primary XANES feature of tetrahedral coordination Al is often at *ca* 1566 eV whilst the primary feature of octahedral coordination Al is at *ca* 1568 or 1571 eV (*i.e.* 2 to 5 eV higher than for tetrahedral coordination Al) (Hu *et al.*, 2008). Furthermore, although Al that is tetrahedrally coordinated has only weak features at energies higher than its main feature, octahedrally coordinated Al often has strong features at higher energies. Finally, slight variations in observed spectral features (such as slight shifts in peak position and shape) are a reflection of the influence of second neighbours and the distribution of Al–O distances (Zhang *et al.*, 2009).

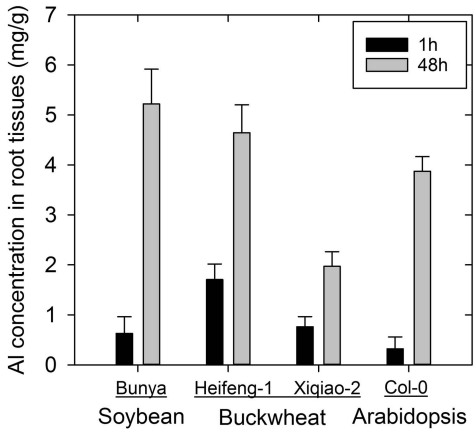

Figure 2
Concentrations of Al (dry-weight basis) in apical (0–10 mm) root tissues of soybean, buckwheat and Arabidopsis. Roots were exposed to Al for either 1 or 48 h. The solutions contained Al at different concentrations: 30 μ*M* Al for soybean (Bunya) (causing 75% reduction in RRER over 48 h), 120 μ*M* for buckwheat Heifeng-1 (25% reduction), 50 μ*M* for buckwheat Xiqiao-2 (25% reduction) and 36 μ*M* for Arabidopsis (Col-0) (60% reduction).

First, we compared differences between the Al *K*-edge XANES spectra of the nine standard compounds (Fig. 3). As reported previously for inorganic Al minerals (Ildefonse *et al.*, 1998; Hu *et al.*, 2008; Zhang *et al.*, 2009), two broad groups could be identified. Compounds containing tetrahedrally coordinated Al had a main feature at *ca* 1566 eV, such as Al–phosphate (Fig. 3). In contrast, compounds containing octahedral coordination Al had a main feature at *ca* 1568 to 1571 eV, including gibbsite, Al–malate, Al–oxalate and Al–pectin. For γ-Al_2O_3, distinct peaks were observed at 1565.8, 1567.1 and 1570.5 eV, as this compound has both tetrahedrally and octahedrally coordinated Al (Fig. 3). Finally, the spectra for hydroxyaluminosilicate was somewhat similar to that of γ-Al_2O_3, with peaks at 1567.1 and 1570.5 eV being indicative of both tetrahedrally and octahedrally coordinated Al (Fig. 3).

Of particular interest in the present study were some of the compounds with octahedral coordination, *i.e.* Al–malate, Al–oxalate and Al–pectin. These compounds are known to be important in regard to the speciation of Al in plant tissues. The spectra of these three compounds were found to be generally similar, with a strong broad single peak at *ca* 1569 eV (Fig. 3). Firstly, comparing Al–malate and Al–oxalate, the spectra were unsurprisingly markedly similar, with the peak for Al–oxalate being slightly broader than for Al–malate (Fig. 3). Compared with Al–malate and Al–oxalate, Al–pectin tended to have a slightly broader peak yet again (Figs. 3 and S4 in the supporting information). However, for the Al–pectin compounds, a small shoulder (low-intensity peak) was observed at an energy of 1565 eV indicating the presence of some Al that is tetrahedrally coordinated (Fig. 3). Finally, for these Al–pectin compounds, differing the proportion of the negative charge saturated by Al (from 50 to 150%) did not markedly alter the spectra obtained (Fig. 3).

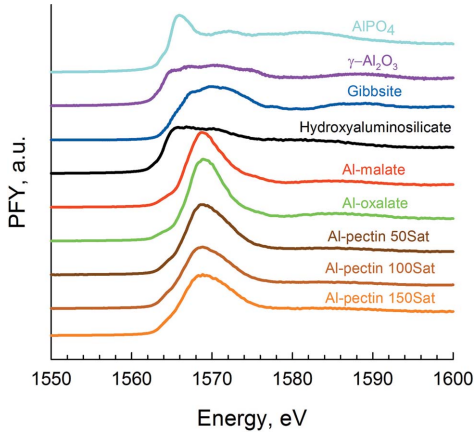

Figure 3
In situ Al *K*-edge XANES spectra for nine Al standard compounds obtained using synchrotron-based XAS. 50Sat is 50% saturation, 100Sat is 100% saturation and 150Sat is 150% saturation. PFY = partial fluorescence yield.

3.3. Al *K*-edge XANES in root tissues

Firstly, the Al *K*-edge spectra were compared between the three plant species for root tissues following exposure to Al for 48 h (Figs. 4 and S1). It was determined that the spectra obtained for buckwheat were similar to those of Al–malate, Al–oxalate and Al–pectin, with the main feature at *ca* 1569 eV indicating the presence of octahedrally coordinated Al (Figs. 4 and S1). Indeed, for both of these plant species, the spectral features (Fig. 4) were visually similar to those of Al–malate, Al–oxalate and Al–pectin (Figs. 4 and S2). Given the error associated with measurement of these root tissues with low Al concentrations (compare the noise for the root spectra to that of the standard compounds, Figs 3 and 4), it was not possible to determine which of these three standard compounds most closely matched the spectra for soybean and buckwheat (Figs. 3 and S2).

In contrast to these two plant species, the Al *K*-edge XANES spectra for roots of Arabidopsis exposed to Al for 48 h generally had a well defined main peak at 1567 eV in addition to a smaller peak at 1571 eV [Figs. 4(*c*) and S3]. This well defined main peak at 1567 eV was 2 eV lower than that observed for octahedrally coordinated Al–malate, Al–oxalate and Al–pectin, but it was also 1 eV higher than that observed for tetrahedrally coordinated Al–phosphate. Indeed, neither the main peak at 1567 eV nor the smaller peak at 1571 eV corresponded to any of the nine Al standards analyzed in the current experiment (Figs. 3, 4, and S3). However, the spectral features of Arabidopsis matched with those of α-Al_2O_3 (corundum) reported by Ildefonse *et al.* (1998), with peaks at 1567.4 and 1571.6 eV. We also compared changes in the Al *K*-edge of roots spectra over time for both soybean and buckwheat (ranging from 1 to 48 h exposure). However, no notable changes were observed for any of the three plant species, with only subtle differences between the spectra (Fig. 4).

Finally, for the LCF, we used the *K*-edge reference for Al–phosphate, γ-Al_2O_3, hydroxyaluminosilicate, Al–malate, Al–oxalate and Al–pectin (50, 100 and 150% saturated). Given that the spectra for Al–malate, Al–oxalate and Al–pectin were similar and could not be easily distinguished from each other,

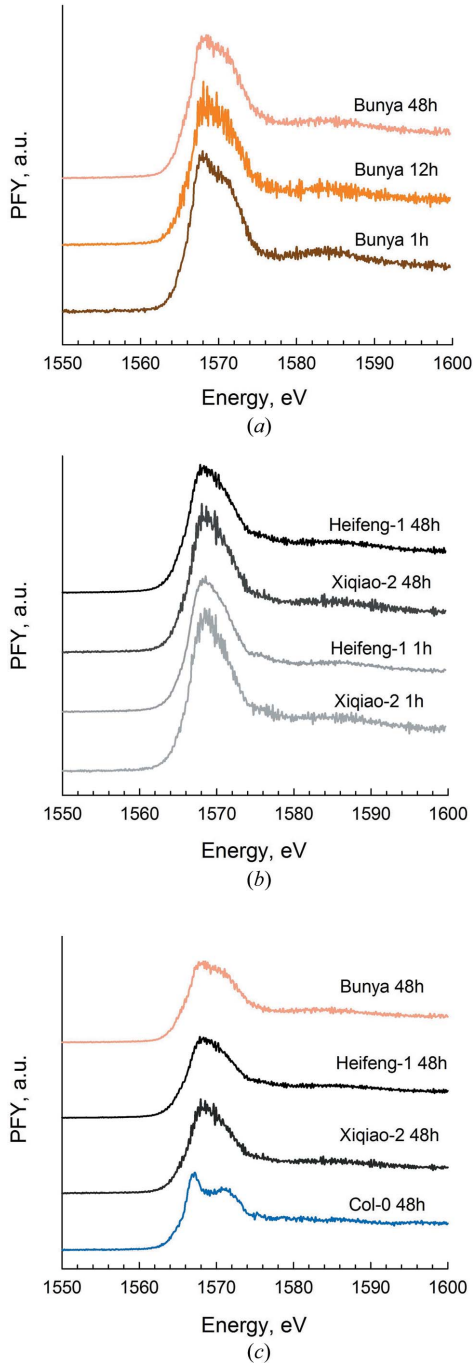

Figure 4
In situ K-edge XANES spectra obtained for the root tissues of three plant species obtained using synchrotron-based XAS. Data are presented for soybean (Bunya) (*a*), buckwheat (Heifeng-1 and Xiqiao-2) (*b*) and Arabidopsis (Col-0) (*c*) exposed to Al for 1, 12 or 48 h. The Al concentrations in the rooting media were sufficient to reduce soybean RRER by 75%, reduce buckwheat RRER by 25% and reduce Arabidopsis RRER by 60% over 48 h. PFY = partial fluorescence yield.

only Al–malate was used in the LCF, with this hereafter referred to as carboxyl–Al in regard to the LCF. For soybean, carboxyl–Al was predicted to account for 94.6% of the Al in the tissues (Fig. S5 and Table S1 in the supporting information). However, it was apparent that the fit was not optimal, with the peak for the sample being much broader than that predicted using LCF (Fig. S5). For buckwheat, the fit predicted by LCF was considerably better (Fig. S6 and Table S1), with 95.6% of the Al predicted to be carboxyl–Al. For Arabidopsis, the *R* value (0.051, Table S1) indicated a markedly poor fit, with the reference standards used in the present study not able to describe the Al speciation in the Arabidopsis tissues (Fig. S7).

3.4. Al *L*-edge XANES in standard compounds and root tissues

We examined the suitability of Al *L*-edge analyses for differentiating between the standard compounds and the forms of Al in the root tissues (Fig. 5). The spectra from the Al *L*-edge are known to be more sensitive than the Al *K*-edge to the chemical environment, providing information on the coordination state of the Al and the nature of the chemical bonding (Weigel *et al.*, 2008). For example, a decrease in the Al coordination results in a shift to lower energy, with the Al *L*-edge spectra usually dominated by two features because of transitions from the Al 2*p* bonding electrons to the Al 3*s* and 3*d* orbitals. The lower-energy transition ($2p^5 3s^*$) can be split into multiple peaks (referred to as the L_3 and L_2 edges) (for example, $AlPO_4$), mainly dependent on the crystallinity of the material. In contrast, the higher-energy transition ($2p^5 3d^*$) occurs as a broad peak dependent on the amorphism (O'Brien *et al.*, 1991; Weigel *et al.*, 2008; Hu *et al.*, 2008; Xu *et al.*, 2010).

The Al *L*-edge spectra of the $AlPO_4$, γ-Al_2O_3 and gibbsite [$Al(OH)_3$] used in this study are similar to those previously published (Zhang *et al.*, 2009; Hu *et al.*, 2008). For the $AlPO_4$, γ-Al_2O_3, gibbsite and hydroxyaluminosilicate reference compounds, various differences were observed between the spectra. For example, $AlPO_4$ had peaks at 78.2 and 80.7 eV, γ-Al_2O_3 had peaks at 77.9 and 79.8 eV, while hydroxyaluminosilicate had peaks at 77.6 and 81.4 eV (Fig. 5). For the Al *L*-edge spectra of the Al-organic reference compounds prepared in this study, broad peaks were apparent at around

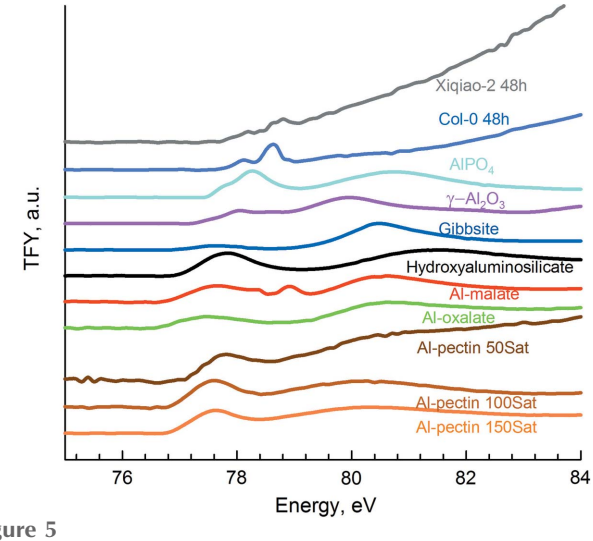

Figure 5
In situ L-edge XANES spectra obtained for nine standard compounds and the selected plant samples obtained using synchrotron-based XAS. Data are presented for buckwheat (Xiqiao-2) and Arabidopsis (Col-0) exposed to Al for 48 h. 50Sat is 50% saturation, 100Sat is 100% saturation and 150Sat is 150% saturation. TFY = total fluorescence yield.

77.5 and 80.3 eV, which is indicative of amorphous Al-organic materials. However, for the Al–malate standard compound, two additional sharp peaks in the $L_{2,3}$-region were observed at higher energy (78.2 and 78.8 eV) on top of the broad peak (Fig. 5). For the different Al–pectin compounds with different degrees of saturation, the peak was at 77.5 eV for the pectin at 100 and 150% saturation, but at 77.6 eV for the pectin at 50% saturation.

Two selected plant samples with high concentrations, buckwheat (Xiqiao-2) and Arabidopsis (Col-0), were analyzed at the *L*-edge, examined after 48 h of Al exposure. Given the poorer detection limit at the *L*-edge (or needs high-concentrated samples), it was not possible to examine plant tissues with shorter periods of exposure. It was found that the spectra of both plant samples exposed to Al for 48 h had peaks at ~78.2 and 78.8 eV, which were located in the Al $L_{2,3}$ region (Fig. 5). The spectra of the two samples were not similar to that of $AlPO_4$, γ-Al_2O_3 and gibbsite, nor to that of three types of Al–pectin with different saturation degree. However, the spectra of the two samples were observed to have the same feature as Al–malate (Fig. 5).

4. Discussion

Synchrotron-based approaches are being used increasingly to investigate complex problems within the plant and soil sciences (Lombi & Susini, 2009). However, despite the global importance of Al toxicity in acid soils, few studies have investigated the potential usefulness of such approaches for the investigation of Al distribution and speciation in plant tissues. Tolrà *et al.* (2011) utilized low-energy X-ray fluorescence (LEXRF) to investigate the distribution of Al in leaves of tea (*Camellia sinensis*), finding that Al generally accumulated in the cell wall. Similarly, Kopittke *et al.* (2015) utilized LEXRF to examine the Al distribution in roots of soybean exposed to Al for 0.5 to 24 h. However, other than Kopittke, Wang *et al.* (2017), we are not aware of any studies that have investigated the suitability of synchrotron-based XANES for examining the speciation of Al in plant tissues, as used for examining the speciation of Al in soil minerals (Ildefonse *et al.*, 1998; Li *et al.*, 1995; Hu *et al.*, 2008; Xu *et al.*, 2010). Rather, studies in plant sciences have generally utilized synchrotron-based approaches for studies of Mn, Fe, Ni, Cu, Zn and As, amongst others (Lombi & Susini, 2009; Singh & Grafe, 2010).

4.1. Use of Al *K*-edge XANES

In the present study, the Al *K*-edge XANES spectra from nine standard compounds were compared. As reported previously for Al minerals, *K*-edge XANES was found to be useful for the separation of tetrahedrally and octahedrally coordinated environments, with the *K*-edge peak moving to higher energies with increasing coordination number (Fig. 3) (Ildefonse *et al.*, 1998; Xu *et al.*, 2010; Hu *et al.*, 2008). However, of the compounds considered more likely to form within plant tissues, Al–malate, Al–oxalate and Al–pectin (octahedrally coordinated) all had largely similar *K*-edge spectra, making the differentiation between these important compounds difficult. The similarities between these compounds are perhaps not unexpected given that Al binding for all of these compounds is through carboxyl groups. However, because of its low solubility, Al–phosphate is also potentially of importance within plant tissues (Batty *et al.*, 2002; Shen *et al.*, 2011), with the spectra of this (tetrahedrally coordinated) compound differing markedly from the others (Fig. 3).

For the plant root tissue samples, the *K*-edge XANES spectra were similar for both soybean and buckwheat, with the spectra of these two species differing from Arabidopsis (Figs. 4 and S3). Importantly, for soybean and buckwheat, the spectra were similar to those of Al–malate, Al–oxalate and Al–pectin, suggesting the likely importance of carboxyl groups for the complexation of Al in the root tissues of these two species (Figs. 3, 4 and S2). Unfortunately, however, the current approach does not permit detailed identification of the precise speciation of similar forms of Al. For example, it is known that the binding of Al to pectin is associated with toxicity, including in soybean (Kopittke *et al.*, 2015) and in wheat (Jones *et al.*, 2006), whilst the binding by simple organic acids is associated with detoxification of Al, including in buckwheat (Ma *et al.*, 1998) and in wheat (*T. aestivum*) (Delhaize *et al.*, 1993). The apparent inability of Al *K*-edge XANES to differentiate between some of these physiologically relevant forms of Al would thus limit its suitability for the investigation of Al in plant tissues in some studies.

For Arabidopsis, it was found that the spectra differed substantially from soybean and buckwheat, with a well defined main peak at 1567 eV in addition to a smaller peak at 1571 eV (Fig. 4). Despite these differences, the spectra for the roots of Arabidopsis did not closely match with any of the nine standard compounds examined in the present study. Although it is possible that the plant tissues analyzed were contaminated by Al associated with agar, it is considered unlikely given that agar is derived from the polysaccharide agarose from the cell wall of algae (Lahaye *et al.*, 1986). Thus, although not tested in the present experiment, Al–agar would be expected to have a XANES spectra similar to that found for Al–pectin. Further work is required in order to determine the speciation of Al in the roots of Arabidopsis.

Thus, in the present study, we have found that, although suitable for distinguishing between Al that is tetrahedrally and octahedrally coordinated, *K*-edge XANES does not appear to be suitable for separating Al binding to some common physiologically relevant compounds within plant tissues (*i.e.* pectin and simple organic acids). However, where there are marked changes in the forms of Al within plant roots (for example, tetrahedrally *versus* octahedrally coordinated), *K*-edge XANES would be suitable in separating these differences. In this regard, Kopittke, McKenna *et al.* (2017) found differences in the tetrahedrally and octahedrally coordinated Al in root tissues of wheat NILs, with this providing valuable information in this previous study. Furthermore, *K*-edge XANES may be suitable to complement other analyses, such as ^{27}Al nuclear magnetic resonance (NMR). However, NMR

has a comparatively poor detection limit and has generally only been used for the investigation of Al accumulators (Ma *et al.*, 1997; Morita *et al.*, 2008).

4.2. Use of Al *L*-edge XANES

The *L*-edge spectra of the Al–pectin, Al–oxalate and Al–malate materials exhibited two broad peaks, at 77.5 and 80.3 eV for Al-pectin, and at 77.5 and 80.6 eV for Al–oxalate and Al–malate (Fig. 5). These peaks are attributed to the amorphous nature of the Al in these compounds. Thus, Al *L*-edge XANES would appear to be potentially suitable, at least to some extent, for the *in situ* differentiation between Al bound to pectin and Al bound to simple organic acids. In other studies, Al-organic materials (Al–tannate, Al–oxalate, Al–malate, Al–acetate and Al–salicylate) (Xu *et al.*, 2010; Hu *et al.*, 2008) and Al–carbonate (Zhang *et al.*, 2009) also showed two broad peaks, with slight shifts in the energy position.

The spectra of the Al–malate standard prepared in this study showed not only the two broad peaks expected for an Al–malate material (Fig. 5) but also two other $L_{2,3}$ peaks (Fig. 5). This indicated that there was also another Al compound that had formed in the Al–malate material. From previous studies, for example O'Brien *et al.* (1991) and Weigel *et al.* (2008), the peak appears to correspond to that observed for α-Al_2O_3, but this is unlikely as the formation of Al oxides requires high temperatures (Wefers & Misra, 1987; Hsu, 1989). Interestingly, however, it has been reported that crystalline Al–malate forms at malate/Al molar ratios (MRs) of 1:1 and 2:1 at low pH and at room temperature (Happel *et al.*, 2007). Indeed, the conditions used in the present study for the preparation of the Al–malate materials differed from the methods used by Xu *et al.* (2010). The Al–malate materials prepared in this study had a MR of 5.0 and the pH was maintained at 4.5 for 48 h, while for the Xu *et al.* (2010) study the malate/Al MR was 0.001, 0.01 and 0.1 and prepared at a pH of ∼9, and after ageing for 40 d the pH was *ca* 6.7. In the study by Xu *et al.* (2010), gibbsite, bayerite and/or pseudo-boehmite were present in the malate/Al MR 0.001 and 0.01 materials along with an amorphous Al–malate, while in the malate/Al MR of 0.1 the materials were amorphous. Thus, we examined whether it was crystalline or amorphous form. It was then determined as amorphous form by collecting the XRD pattern of the Al–malate sample.

Interestingly, it appears that the Al from the samples was present as a crystalline material as evident by the two peaks in the $L_{2,3}$ region of the Al *L*-edge spectra (78.2 and 78.8 eV, Fig. 5). Several points are important in regard to this observation of crystalline materials in the root tissue samples. It is not possible to determine if the formation of a crystalline material in the plant root tissues occurred during plant growth or if it occurred as an experimental artefact after harvest during the freezing and subsequent freeze drying, but we contend that this should be further examined. Unfortunately, because of their low energy values, both Al *K*-edge and Al *L*-edge analyses must be performed in the vacuum, which necessitates sample processing and dehydration. In this regard, although we observed crystalline Al in the plant root tissues, we do not suggest that the crystalline Al in the root tissues is necessarily any of the standard compounds studied in this research. Rather, we contend that the exact form of crystalline Al in the root tissues remains unclear.

Of further interest for the *L*-edge XANES, there were slight variations in the energy values corresponding to peaks of pectin and the peaks of Al–oxalate and Al–malate as discussed earlier (Fig. 5). Thus, in this regard, Al *L*-edge analyses would appear to be potentially useful for the differentiation of these compounds. Unfortunately, for the plant tissues, this broad peak at higher energies (*ca* 80.3–80.6 eV) was not readily evident, thus preventing the differentiation between these compounds in this study. This higher-energy peak could not be readily observed because of the sloping background of the Al *L*-edge spectra, which at the low Al concentrations of the root tissues obscured the peak (Fig. 5). This effect of Al concentration on the normalization of the Al *L*-edge spectra was also evident from the Al–pectin series, where the broad peak at higher energy was difficult to see in the Al–pectin at 50% saturation in contrast to the Al–pectin at 100 and 150% saturation, again because of normalization (Fig. 5). It is important to note that the reason we do not see differences in the Al–malate *K*-edge spectra (Fig. 3) is presumed to be because both the amorphous and crystalline Al–malate materials are predominantly octahedrally coordinated.

Thus, for Al *L*-edge analyses, the slight shifts in the peaks make it possible to differentiate between physiologically relevant forms of Al, such as Al–pectin and Al–malate or Al–oxalate. However, because of the poorer sensitivity of *L*-edge analyses and the comparatively low concentrations of Al in root tissues, it was not possible in the present study to differentiate between these forms of Al in the plant samples. Furthermore, it is possible that the dehydration of plant tissues required to perform these analyses caused the formation of crystalline Al compounds, with *L*-edge analyses differentiating between amorphous and crystalline compounds.

5. Conclusion

In the present study, we have investigated the suitability of both Al *K*- and *L*-edge XANES spectroscopy for the *in situ* examination of the speciation of Al within plant root tissues. Such an approach would be of potential value for understanding the behaviour of Al within plants, including for understanding the mechanism by which Al is toxic to plant roots, as well as for understanding the mechanisms used by some plants to tolerate elevated levels of Al. Three plant species differing in their tolerance to Al were compared, and their *K*-edge and *L*-edge XANES spectra compared with those from various standard compounds. For the *K*-edge, it was found that, although XANES spectroscopy is suitable for differentiating between Al that is tetrahedrally and octahedrally coordinated, the Al *K*-edge XANES was not suitable for separating Al binding to some of the common physiologically

relevant compounds within plant tissues, such as pectin and simple organic acids. This is important given that binding to pectin (cell wall) is associated with the exertion of toxic effects, while the binding to simple organic acids is typically associated with tolerance mechanisms. Next, we examined the suitability of Al *L*-edge XANES spectroscopy. Although this approach is able to provide more information on the nature of the chemical bonding than the *K*-edge, it has a higher (poorer) detection limit, which hinders its use in plant tissues (in which Al concentrations are lower than in soil minerals, for example). Indeed, although *L*-edge analyses are able to differentiate between physiologically relevant forms of Al, such as Al–pectin and Al bound to simple organic acids (such as Al–malate or Al–oxalate), the low concentration of Al in plant root tissues prevented this differentiation. Furthermore, it is possible that the dehydration of plant roots required for these *in situ* analyses resulted in the formation of a crystalline Al compound, with *L*-edge analyses being sensitive to crystalline and amorphous forms of Al. Thus, overall, our data suggest that Al *K*-edge analyses can be used to differentiate between tetrahedrally and octahedrally coordinated Al in plant tissues, but the poorer sensitivity of the *L*-edge analyses unfortunately limits the versatility of this approach in plant tissues where concentrations are low compared with other samples, such as Al-containing minerals.

Acknowledgements

The authors would like to thank Professor Chaofen Huang for providing buckwheat seeds and Joel Reid for diffraction tests.

Funding information

We thank the International Synchrotron Access Program (ISAP) managed by the Australian Synchrotron, part of ANSTO, and the Australian Government. Part of the research described in this article was performed at the Canadian Light Source, which is supported by the Canada Foundation for Innovation, the Natural Sciences and Engineering Research Council of Canada, the University of Saskatchewan, the Government of Saskatchewan, Western Economic Diversification Canada, the National Research Council of Canada, and the Canadian Institutes of Health Research. Zhigen Li is a recipient of a scholarship from the China Scholarship Council (201506300048) and is a recipient of The University of Queensland International Scholarship (UQI). Dr Kopittke is the recipient of an Australian Research Council (ARC) Future Fellowship (FT120100277) and Dr Wang is the recipient of an ARC Discovery Early Career Researcher Award (DECRA, DE130100943).

References

Batty, L. C., Baker, A. J. & Wheeler, B. D. (2002). *Ann. Bot.* **89**, 443–449.
Bennet, R., Breen, C. & Fey, M. (1985). *S. Afr. J. Plant. Soil*, **2**, 1–7.
Brevik, E. C. & Burgess, L. C. (2012). *Soils and Human Health*, 1st ed. Boca Raton: CRC Press.
Delhaize, E., Ryan, P. R. & Randall, P. J. (1993). *Plant Physiol.* **103**, 695–702.
Exley, C. & Birchall, J. (1992). *Polyhedron*, **11**, 1901–1907.
Hajkowicz, S. & Young, M. (2005). *Land Degrad. Dev.* **16**, 417–433.
Happel, O., Harms, K. & Seubert, A. (2007). *Z. Anorg. Allg. Chem.* **633**, 1952–1958.
Horst, W. J., Wang, Y. & Eticha, D. (2010). *Ann. Bot.* **106**, 185–197.
Hsu, P. H. (1989). *Aluminum Oxides and Oxyhydroxides*, edited by J. B. Dixon and S. B. Weed, pp. 331–378. Madison: Soil Science Society of America.
Hu, Y., Xu, R., Dynes, J., Blyth, R., Yu, G., Kozak, L. & Huang, P. (2008). *Geochim. Cosmochim. Acta*, **72**, 1959–1969.
Hu, Y. F., Zuin, L., Wright, G., Igarashi, R., McKibben, M., Wilson, T., Chen, S. Y., Johnson, T., Maxwell, D., Yates, B. W., Sham, T. K. & Reininger, R. (2007). *Rev. Sci. Instrum.* **78**, 083109.
Huang, C. F., Yamaji, N. & Ma, J. F. (2010). *Plant Physiol.* **153**, 1669–1677.
Ildefonse, P., Cabaret, D., Sainctavit, P., Calas, G., Flank, A. M. & Lagarde, P. (1998). *Phys. Chem. Miner.* **25**, 112–121.
Ishikawa, S., Wagatsuma, T., Sasaki, R. & Ofei-Manu, P. (2000). *Soil Sci. Plant Nutr.* **46**, 751–758.
Jones, D., Blancaflor, E., Kochian, L. & Gilroy, S. (2006). *Plant Cell Environ.* **29**, 1309–1318.
Kasrai, M., Yin, Z., Bancroft, G. M. & Tan, K. H. (1993). *J. Vac. Sci. Technol. A*, **11**, 2694–2699.
Kerven, G., Edwards, D., Asher, C., Hallman, P. & Kokot, S. (1989). *Soil Res.* **27**, 91–102.
Kopittke, P. M., McKenna, B. A., Karunakaran, C., Dynes, J. J., Arthur, Z., Gianoncelli, A., Kourousias, G., Menzies, N. W., Ryan, P. R., Wang, P., Green, K. & Blamey, F. P. C. (2017). *Front. Plant Sci.* **8**, 1377.
Kopittke, P. M., Menzies, N. W., Wang, P. & Blamey, F. P. C. (2016). *J. Exp. Bot.* **67**, 4451–4467.
Kopittke, P. M., Moore, K. L., Lombi, E., Gianoncelli, A., Ferguson, B. J., Blamey, F. P. C., Menzies, N. W., Nicholson, T. M., McKenna, B. A., Wang, P., Gresshoff, P. M., Kourousias, G., Webb, R. I., Green, K. & Tollenaere, A. (2015). *Plant Physiol.* **167**, 1402–1411.
Kopittke, P. M., Wang, P., Lombi, E. & Donner, E. (2017). *J. Environ. Qual.* **46**, 1175–1189.
Lahaye, M., Rochas, C. & Yaphe, W. (1986). *Can. J. Bot.* **64**, 579–585.
Larsen, P. B., Geisler, M. J., Jones, C. A., Williams, K. M. & Cancel, J. D. (2005). *Plant J.* **41**, 353–363.
Li, D., Bancroft, G., Fleet, M., Feng, X. & Pan, Y. (1995). *Am. Mineral.* **80**, 432–440.
Liu, Q., Golubovskaya, I. & Cande, W. Z. (1993). *J. Cell Sci.* **106**, 1169–1178.
Lombi, E. & Susini, J. (2009). *Plant Soil*, **320**, 1–35.
Ma, J. F., Hiradate, S. & Matsumoto, H. (1998). *Plant Physiol.* **117**, 753–759.
Ma, J. F., Zheng, S. J., Matsumoto, H. & Hiradate, S. (1997). *Nature*, **390**, 569–570.
McKenna, B. A., Kopittke, P. M., Wehr, J. B., Blamey, F. P. C. & Menzies, N. W. (2010). *Physiol. Plant.* **138**, 205–214.
Morita, A., Yanagisawa, O., Takatsu, S., Maeda, S. & Hiradate, S. (2008). *Phytochemistry*, **69**, 147–153.
NLWRA (2002). *Australian Catchment, River and Estuary Assessment 2002.* National Land and Water Resources Audit, Canberra, Australia.
O'Brien, W. L., Jia, J., Dong, Q. Y., Callcott, T. A., Rubensson, J. E., Mueller, D. L. & Ederer, D. L. (1991). *Nucl. Instrum. Methods Phys. Res. B*, **56–57**, 320–323.
Shen, J., Yuan, L., Zhang, J., Li, H., Bai, Z., Chen, X., Zhang, W. & Zhang, F. (2011). *Plant Physiol.* **156**, 997–1005.
Singh, B. & Grafe, M. (2010). *Synchrotron-Based Techniques in Soils and Sediments*, 1st ed, Vol. 34. Amsterdam: Elsevier.
Sivaguru, M. & Horst, W. J. (1998). *Plant Physiol.* **116**, 155–163.

Sposito, G. (2008). *The Chemistry of Soils*, 2nd ed. New York: Oxford University Press.
Taylor, G. J., McDonald-Stephens, J. L., Hunter, D. B., Bertsch, P. M., Elmore, D., Rengel, Z. & Reid, R. J. (2000). *Plant Physiol.* **123**, 987–996.
Tolrà, R., Vogel-Mikuš, K., Hajiboland, R., Kump, P., Pongrac, P., Kaulich, B., Gianoncelli, A., Babin, V., Barceló, J., Regvar, M. & Poschenrieder, C. (2011). *J. Plant Res.* **124**, 165–172.
Uexküll, H. R. von & Mutert, E. (1995). *Plant Soil*, **171**, 1–15.
Wefers, K. & Misra, C. (1987). *Oxides and Hydroxides of Aluminum*, Alcoa Technical Paper No. 19 Revised. Aluminum Company of America, Pittsburgh, Pennsylvania, USA.
Weigel, C., Calas, G., Cormier, L., Galoisy, L. & Henderson, G. (2008). *J. Phys. Condens. Matter*, **20**, 135219.
Xu, R., Hu, Y., Dynes, J., Zhao, A., Blyth, R., Kozak, L. & Huang, P. (2010). *Geochim. Cosmochim. Acta*, **74**, 6422–6435.
Yamamoto, Y., Kobayashi, Y., Devi, S. R., Rikiishi, S. & Matsumoto, H. (2002). *Plant Physiol.* **128**, 63–72.
Yamamoto, Y., Kobayashi, Y. & Matsumoto, H. (2001). *Plant Physiol.* **125**, 199–208.
Zhang, G., Hu, Y., Xu, R., Dynes, J., Blyth, R., Kozak, L. & Huang, P. (2009). *Clays Clay Miner.* **57**, 795–807.
Zhu, H. F., Wang, H., Zhu, Y. F., Zou, J. W., Zhao, F. J. & Huang, C. F. (2015). *BMC Plant Biol.* **15**, 16.